A 20 GHz Steerable Array Antenna Using 3-bit Dielectric Slab Phase Shifters on a Coplanar Waveguide

Junho Cha, *Member, IEEE*, Yasuo Kuga, *Fellow, IEEE*, Akira Ishimaru, *Life Fellow, IEEE*, and Sangil Lee

***Abstract*—A simple steerable array antenna is designed and developed using a movable dielectric phase shifter. The change of effective dielectric constant at different dielectric slab positions on a coplanar waveguide is used as the phase shifter. The impedance matching and desired phase shift conditions are satisfied at two slab heights, and the reflection is designed to be minimized at these slab positions. The low-loss dielectric material is used as the dielectric slab and is placed close to a coplanar transmission line with airgap. The 4 × 4 steerable array antenna with the phase shifters is designed and fabricated at 20 GHz. The H-plane radiation patterns are measured at different phase shift positions and compared with the expected results.**

***Index Terms*—Coplanar waveguide, phase shifter, steerable array antenna.**

I. Introduction

THE global satellite systems play a significant role in civilian and military communications. Currently, several military communication systems are using the *K*- and *Ka*-band frequencies (18–40 GHz). Although the initial attempt by Teledesic was not successful, it is expected that deployment of high-speed satellite-based communication links will be inevitable in the future. The current low-data rate satellite phones such as Iridium will have a limited use as a high-speed data link. One of the problems of Teledesic was the expected high cost of a ground station which can track the low-earth orbit (LEO) satellites. We believe that a low-cost steerable antenna is one of the missing links for the future of flexible wireless communication systems. The most flexible satellite-to-ground communication system is based on electronic phased-array antenna technology [1]. However, the cost of a phased-array antenna is related to the number of active elements, and thus the present systems are often too expensive for many commercial and military applications. The antenna beam steering can also be done by mechanically moving the reflector or lens [2]. Although the mechanically steerable antennas can be less expensive than the electric phased-array antennas, the electromechanical actuators/motors are usually bulky and prone to mechanical failure.

The phase shifters are a critical element for electronically scanned phased-array antennas, and typically account for a significant amount of the cost of producing an antenna array. The reduction of fabrication cost opens possibilities for many applications. Recently, the different types of microwave phase shifters including MEMS-based and ferroelectric-based, have been proposed for antenna applications [3], [4]. In addition, a phase shifter using a PZT controlled dielectric layer to perturb the electromagnetic fields of a CPW has been demonstrated [5]. In this paper, we introduce that a movable dielectric slab which is placed close to a coplanar waveguide (CPW) with airgap can be used as a phase shifter. We minimize the refection with or without dielectric material (ON-OFF position) at the designed frequency. The proposed array antenna consists of the series-fed patch antennas, phase shifters, and the feeding network as shown in Fig. 1. It is noted that the most difficult part of our design, simulation and fabrication processes is the phase shifter [6]. The desired phase shift may not be achievable with all transmission line (TL) types. To obtain the optimum combinations of the TL structure and dielectric material, we have investigated several TL structures. These include a microstrip TL, CPW TL without airgaps, and CPW TL with airgaps. Our studies show that the microstrip TL and CPW TL without airgaps are insensitive to the presence of a dielectric slab on them and are eliminated from consideration. In addition, it is found that a high-ε_r material such as $BaTiO_3$ is not suited for a phase shifter. It appears that the electromagnetic field perturbation caused by a high-ε_r material is significant, and the structure does not work as a phase shifter. The best dielectric materials seem to be in the range of $\varepsilon_r = 3$ to 10 in our case. Because we are introducing the impedance mismatch section on TL, the elimination of reflection is essential to design a phase shifter, and possible solutions for the impedance mismatch problems are explored [7]. To minimize the reflection caused by the dielectric slab and also obtain the desired phase shifter, the dielectric constant of the slab has to be set to a specific value. The performance of the CPW-based phase shifter was tested at 6 GHz. Fig. 1 shows the final layout of the antenna designed at 20 GHz. Using a 3-bit phase shifter, the antenna beam angle can be scanned from $-45°$ to $+45°$. Details will be discussed in the following sections.

II. Phase Shifter Based on a Movable Dielectric Slab

The basic concept of the phase shifter is illustrated in Fig. 2. The CPW has airgaps between the center signal line and ground lines. As the movable dielectric slab moves closer or into the gap of the CPW, the effective dielectric constant changes and is given as a function of d for the given structure. In this paper,

Manuscript received May 15, 2006; revised October 9, 2006. This work was supported by the National Science Foundation under Grant ECS-0424414.

The authors are with the Department of Electrical Engineering, University of Washington, Seattle, WA 98195 USA (e-mail: junho2@u.washington.edu).

Color versions of one or more of the figures in this paper are available online at http://ieeexplore.ieee.org.

Digital Object Identifier 10.1109/TAP.2006.889837

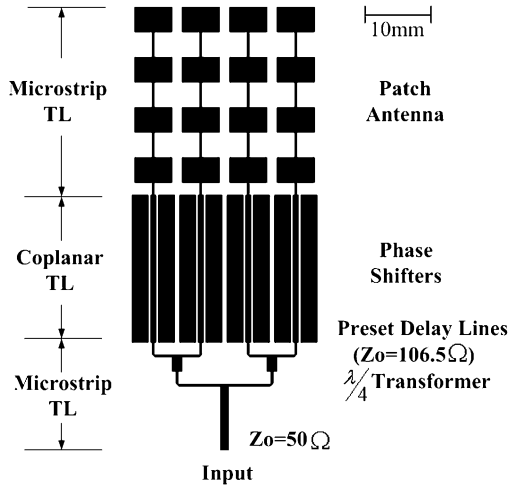

Fig. 1. Block diagram of a 4 × 4 steerable array antenna.

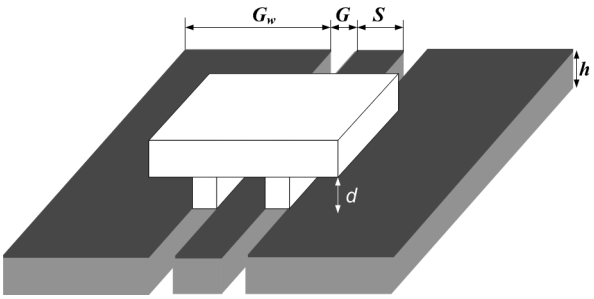

Fig. 2. Phase Shifter. A 3-D schematic of a ground-signal-ground (G-S-G) CPW with a movable dielectric slab. The width of the signal and ground traces are S and G_W, respectively. The gap between the ground and the signal is G and the substrate thickness is h. The height of the dielectric material is 2.5 mm and its length is l.

we assume that the slab can be either attached on the substrate ($d = 0$ or very small) or far away from the substrate ($d = \infty$ or $d > 5$ mm in our case).

This structure can be modeled as an unmatched TL section (or a layered structure). The transmission coefficient T of a layered structure is given as [8]

$$T = \frac{(1-\Gamma_1^2)e^{-j\theta}}{1-\Gamma_1^2 e^{-2j\theta}} \tag{1}$$

where Γ_1 is the reflection coefficient at the boundary due to a semi-infinite layer and θ is the phase shift due to a slab. When θ becomes $m\pi$ where m is an integer, the reflection from the slab diminishes (or $|T|$ becomes 1). This is the impedance matching condition which can also be stated in terms of the effective slab length of $m\lambda/2$. The slab length must satisfy this condition to minimize reflection. In addition, when d is changed from $d = \infty$ to $d = 0$, the phase shift of the slab section will be related to the effective dielectric constant of these two states [9]. Therefore, if we want to create a desired phase shift without creating undesired reflection, we need to satisfy specific conditions for each slab.

A. Impedance Mismatch and Possible Solutions

Suppose we want a 3-bit phase shifter given by 45°, 90° and 180° sections as shown in Fig. 3. Then the available phase shifts

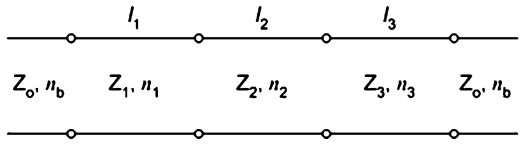

Fig. 3. TL model of a 3-bit phase shifter.

will be eight states (0°, 45°, 90°, 135°, 180°, 225°, 270°, and 315°). The fixed CPW section is denoted by Z_0 and n_b without dielectric slabs. The sections l_1, l_2 and l_3 will have dielectric slabs, and are given by (Z_1, n_1) for $\pi/4$ section, (Z_2, n_2) for $\pi/2$ section and (Z_3, n_3) for π section where Z and n are the characteristic impedance and the index of refraction of each section. We hope to create conditions with no reflection for all states. We also aim to obtain the length l_1, l_2, and l_3 as well as the index of refraction n_1, n_2, and n_3 in terms of n_b. This can be done by satisfying the following conditions.

1) For $\pi/4$ section (45°, bit 0), we need to satisfy

$$(n_1 - n_b)k_0 l_1 = \pi/4 \quad \text{and} \quad n_1 k_0 l_1 = m_1\pi$$

where m_1 is an integer. By eliminating l_1, n_1 is given by

$$n_1 = n_b \frac{4m_1}{4m_1 - 1}. \tag{2}$$

If we choose $m_1 = 1$, then

$$n_1 = \frac{4}{3}n_b \quad \text{and} \quad l_1 = \frac{m_1\pi}{n_1 k_0} = \frac{3}{8}\cdot\frac{\lambda_0}{n_b}. \tag{3}$$

2) For $\pi/2$ section (90°, bit 1), we need to satisfy

$$(n_2 - n_b)k_0 l_2 = \pi/2 \quad \text{and} \quad n_2 k_0 l_2 = m_2\pi$$

where m_2 is an integer. By eliminating l_2, n_2 is given by

$$n_2 = n_b \frac{2m_2}{2m_2 - 1} \tag{4}$$

$$\text{For } m_2 = 1\text{: } n_2 = 2n_b \quad \text{and} \quad l_2 = \frac{\lambda_0}{4n_b} \tag{5}$$

$$\text{For } m_2 = 2\text{: } n_2 = \frac{4}{3}n_b \quad \text{and} \quad l_2 = \frac{3}{4}\frac{\lambda_0}{n_b}. \tag{6}$$

3) For π section (180°, bit 2), we need to satisfy

$$(n_3 - n_b)k_0 l_3 = \pi \quad \text{and} \quad n_3 k_0 l_3 = m_3\pi$$

where m_3 is an integer. By eliminating l_3, n_3 is given by

$$n_3 = n_b \frac{m_3}{m_3 - 1} \tag{7}$$

$$\text{For } m_3 = 2\text{: } n_3 = 2n_b \quad \text{and} \quad l_3 = \frac{1}{2}\cdot\frac{\lambda_0}{n_b} \tag{8}$$

$$\text{For } m_3 = 4\text{:} n_3 = \frac{4}{3}n_b \quad \text{and} \quad l_3 = \frac{3}{2}\cdot\frac{\lambda_0}{n_b}. \tag{9}$$

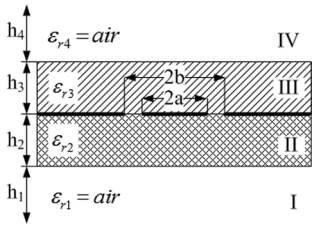

Fig. 4. Frontal view of a ground-signal-ground (G-S-G) CPW ($\varepsilon_{r2} = 3.38$ and $\varepsilon_{r3} = 1$ or 6.2).

4) If we need a $\pi/8$ (22.5°) section for a 4-bit phase shifter, the index refraction n_4 and the length l_4 must satisfy

$$n_4 = n_b \frac{8m_4}{8m_4 - 1} \tag{10}$$

$$\text{For } m_4 = 1, \text{we have } n_4 = \frac{8}{7} n_b \quad \text{and} \quad l_4 = \frac{7}{16} \cdot \frac{\lambda_0}{n_b}. \tag{11}$$

B. Approximate Analytic Formulas for CPW With Dielectric Materials

Next we need to derive a method to obtain the effective dielectric constant of CPW for a given d. The effective dielectric constant of a simple CPW structure has been studied extensively [10]. However, we are unable to find an existing analytical solution for a CPW structure shown in Fig. 2, and we have to rely on the numerical technique.

The previous studies of CPW with dielectric material have the structure shown in Fig. 4. This is similar to our case of $d = 0$. Similarly, when $\varepsilon_{r3} = 1$, the structure is the same as without the dielectric slab case ($d = \infty$). A full-wave analysis of the CPW using Galerkin's method in the spectral domain has been published [11]. Simple analytical formulas for the quasi-TEM parameters were obtained from either exact or approximate conformal mapping techniques. A general CPW with finite width ground planes of the effective dielectric constant and the characteristic impedance are given by [12]

$$\varepsilon_{\text{eff}} = q_1\varepsilon_{r1} + q_2\varepsilon_{r2} + q_3\varepsilon_{r3} + q_4\varepsilon_{r4} \tag{12}$$

$$Z_0 = \frac{1}{c\sqrt{\varepsilon_{\text{eff}} C^a}} \tag{13}$$

where

$$q_1 = \frac{1}{2} - \frac{C^a_{\text{II}}}{C^a}, \quad q_2 = \frac{C^a_{\text{II}}}{C^a}, \quad q_3 = \frac{C^a_{\text{III}}}{C^a}$$
$$q_4 = \frac{1}{2} - \frac{C^a_{\text{III}}}{C^a} \tag{14}$$
$$C^a = 4\varepsilon_0 \frac{K(k_I)}{K'(k_I)}, \quad C^a_i = 2\varepsilon_0 \frac{K(k_i)}{K'(k_i)} \quad (i = \text{I, II, III, and IV})$$
$$K_I = \frac{a}{b}, K_{II} = \frac{\sinh(A_{II})}{\sinh(B_{II})},$$
$$K_{III} = \frac{\sinh(A_{III})}{\sinh(B_{III})}, \quad \text{and}$$
$$K_{IV} = \frac{\tanh(A_{IV})}{\tanh(B_{IV})}$$

TABLE I
COMPARISON WITH APPROXIMATE ANALYTIC FORMULAS AND NUMERICAL RESULTS

	Analytic Formulas		Numerical Results (HFSS)	
Parameters	d=5mm	d=0mm	d=5mm	d=0mm
Characteristic impedance (Ω)	45.37	31.9	39.28	36.9
Effective dielectric constant (ε_{eff})	2.59	5.31	2.63	4.81

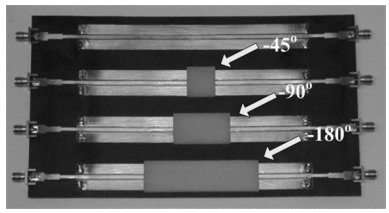

Fig. 5. Phase shifters without (Top TL) and with (Bottom 3 TLs) a dielectric slab.

where

$$A_i = \frac{\pi a}{2h_i}, \quad B_i = \frac{\pi b}{2h_i} \quad (i = \text{I, II, III, and IV})$$
$$q_1 + q_2 + q_3 + q_4 = 1.$$

To check the accuracy of this formula and also the correctness of our simulations, we compared several cases with Ansoft HFSS simulations. Table I shows the comparison of the approximate analytic formulas given in (12) and (13) with the data obtained from HFSS numerical simulations. The agreement is reasonable and our simulation seems to be working. All the following results are obtained using HFSS simulations.

C. Verification of CPW Phase Shifter

In order to verify the validity of this phase shifter, we fabricated the CPW on a Duroid 5880 ($\varepsilon_{\text{sub}} = 2.2$) and measured eight different states. Duroid 5880 was chosen because the dielectric constant is accurately known. Fig. 5 shows the test phase shifter circuits designed at 6 GHz with and without the dielectric slab. The CPW with gap ($Z_0 = 98\ \Omega$) is matched to the mictrostrip TL with $Z_0 = 50\ \Omega$ with $\lambda/4$ transformer for testing purposes. The width of the signal trace S is 2 mm and the width of the ground Gw is 6 mm. The gap G between the ground and the signal is 1 mm. For Duroid 5880, we choose $m_1 = 1, m_2 = 2$, and $m_3 = 4$ so that we can use the same material for all the dielectric slabs. The dielectric slabs must have

$$n_1 = n_2 = n_3 = 4/3n_b, \quad l_1 = 3/8(\lambda_o/n_b),$$
$$l_2 = 3/4(\lambda_o/n_b) \quad \text{and} \quad l_3 = 3/2(\lambda_o/n_b). \tag{15}$$

Since $n_b = 1.23$, the required dielectric constant of the slab is $\varepsilon_r \approx 2.2$. Polyethylene which has $\varepsilon_r = 2.25$, is selected as a dielectric slab material. The lengths of the dielectric slabs which can be obtained using (15) are 15.24 mm, 30.48

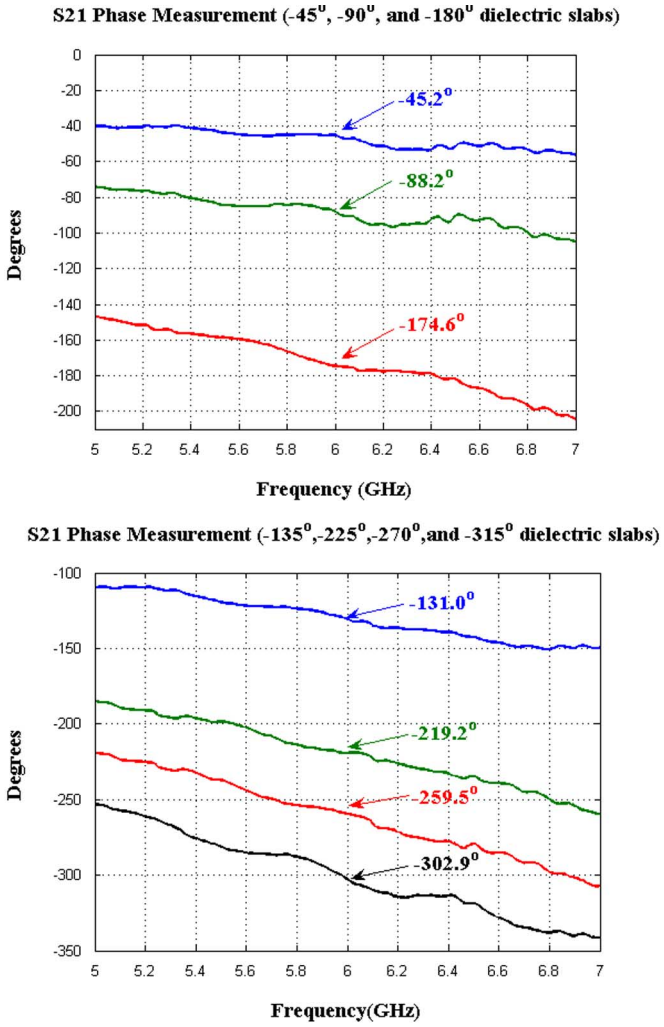

Fig. 6. The measured phase with the 3-bit dielectric slab combinations for the desired eight phase conditions ($0°, -45°, -90°, -135°, -180°, -225°, -270°$, and $-315°$).

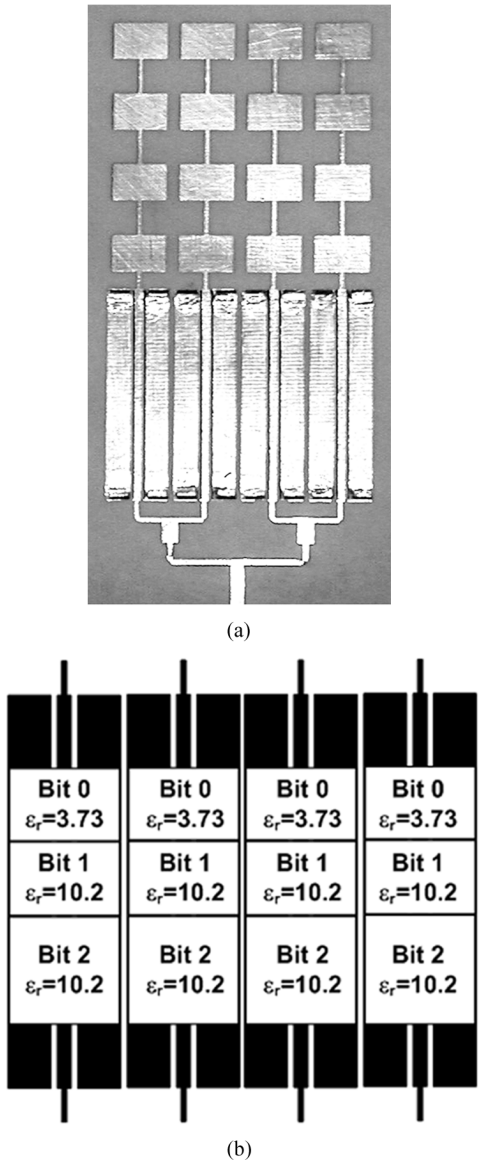

Fig. 7. (a) Layout of a 4×4 array antenna without dielectric slabs. (b) Dielectric slab positions on a CPW for the 3-bit phase shifter.

mm, and 60.97 mm for $-45°, -90°$, and $-180°$ sections, respectively. The height of the dielectric slab is 4 mm and the width is 19 mm. The bottom layer of the CPW section does not have a ground plane and *via* is used for connecting to the ground. Fig. 6 shows the measured phase of S_{21} with the vector network analyzer (VNWA) at seven phase shift positions created by the 3-bit dielectric slab combinations. The measured phase is close to that of the eight phase conditions $(0, -45°, -90°, -135°, -180°, -225°, -270°$, and $-315°)$. The reflections in all cases are small at 6 GHz. This demonstrates that we can design the phase shifter using the dielectric slab on a CPW without introducing impedance mismatch.

III. 4×4 Array Antenna With Phase Shifter at 20 GHz

A low-cost material and fabrication process are among our top design goals. The 20 GHz array antenna and phase shifters are fabricated on the FR-4 based IS640 substrate which is less expensive than Duroid 5880. The characteristics of IS640 are $\varepsilon_r = 3.38, \text{thickness} = 0.508$ mm (20 mil), and loss tangent $= 0.0045$, respectively. To reduce the E-plane beam width, four patch antennas are connected in series as shown in Fig. 7. Although the E-plane side-lobe can be reduced by tapering the patch sizes, it was not included in our design. The antenna patch size is 5.8 mm $\times$ 3.85 mm and the input impedance is 106.5 Ω. The spacing for series elements between edges is 4 mm, and the spacing for patches between center to center is 7.4 mm which is less than 0.5 λ at 20 GHz. The 4×4 array antenna was chosen after testing the E- and H-plane radiation patterns of 4×1, 4×2, and 4×4 array antennas [13], [14]. The E-plane beam size can further be reduced by increasing the number of series elements [15].

The CPW section has a signal line width of S = 0.8 mm, a ground line width of $G_W = 2.5$ mm, and a gap between the signal line and the ground line of $G = 0.4$ mm. The bottom layer of the CPW section does not have a ground plane and *via* is used to connect to the ground. Based on HFSS simulations, it is found that the effective index of refraction without slab is $n_b = 1.152 (\varepsilon_{\text{eff}} = 1.329)$. Ideally, the dielectric slab should fill

TABLE II
SIMULATION RESULTS WITH $\varepsilon_r = 3.73$ SLAB (Slab Length = 4.8 MM)

d (μm)	$\lvert S_{21}\rvert$	$\lvert S_{11}\rvert$	ε_{eff1}
20	0.976	0.073	2.33
19	0.976	0.068	2.341
18	0.976	0.067	2.358
17	0.976	0.064	2.363
16	0.976	0.06	2.375
Air	0.987	0.006	1.329

TABLE III
SIMULATION RESULTS WITH $\varepsilon_r = 10.2$ SLAB (Slab Length = 3.26 MM)

d (μm)	$\lvert S_{21}\rvert$	$\lvert S_{11}\rvert$	ε_{eff2}
8	0.979	0.070	4.936
5	0.982	0.011	5.308
4	0.982	0.02	5.42
3	0.981	0.04	5.57
Air	0.987	0.006	1.329

the gap when $d = 0$ as shown in Fig. 2. Unfortunately, this requires additional costly machining. To reduce processing costs, we investigated the use of slabs without the bottom notches which go into the CPW gaps. The disadvantage of this flat slab is that the effective dielectric constant can be sensitive to a small residual air space and its effect must be included in the simulation. For $\pi/4$ section, we choose $m_1 = 1$ and obtain $n_1 = 1.536$ and $l_1 = 4.48$ mm. The effective dielectric constant of this section must be $\varepsilon_{\text{eff1}} = n_1^2 = 2.359$. To create $\varepsilon_{\text{eff1}} = 2.359$, we use a dielectric material with $\varepsilon_r = 3.73$. Table II shows the effective dielectric constant as a function of residual air space. If a small airgap (10–20 μm) exists between the dielectric slab and the conductor, the dielectric material with $\varepsilon_r = 3.73$ is suitable for 45° sections.

For $\pi/2$ and π sections, we choose $m_2 = 1$ and $m_3 = 2$, and obtain $n_2 = n_3 = 2n_b = 2.305, l_2 = 3.26$ mm, and $l_3 = 6.52$ mm. The effective dielectric constant of these sections must be $\varepsilon_{\text{eff2}} = n_2^2 = 5.316$. To create $\varepsilon_{\text{eff2}} = 5.316$, we use a dielectric material with $\varepsilon_r = 10.2$.

Table III shows the effective dielectric constant as a function of residual air space for the $\pi/2$ section. If a small airgap (5–10 μm) exists between the dielectric slab and the conductor, the dielectric material with $\varepsilon_r = 10.2$ becomes suitable for 90° and 180° sections.

Similarly, if we need a $\pi/8$ section for a 4-bit phase shifter, we choose $m_4 = 1$, and obtain $n_4 = 8/7n_b = 1.316, l_4 = 5.69$ mm. The effective dielectric constant of these sections must be $\varepsilon_{\text{eff4}} = n_4^2 = 1.733$. To create $\varepsilon_{\text{eff4}} = 1.733$, we use a dielectric material with $\varepsilon_r = 2.94$. Table IV shows the effective dielectric constant as a function of residual air space for the $\pi/8$ section. If a small airgap (100–110 μm) exists between the dielectric slab and the conductor, the dielectric material with $\varepsilon_r = 2.94$ is suitable for 22.5° section.

TABLE IV
SIMULATION RESULTS WITH $\varepsilon_r = 2.94$ SLAB (Slab Length = 5.69 MM)

d (μm)	$\lvert S_{21}\rvert$	$\lvert S_{11}\rvert$	ε_{eff4}
90	0.982	0.008	1.77
100	0.982	0.008	1.75
110	0.983	0.007	1.723
115	0.983	0.007	1.71
120	0.983	0.007	1.70
Air	0.987	0.006	1.329

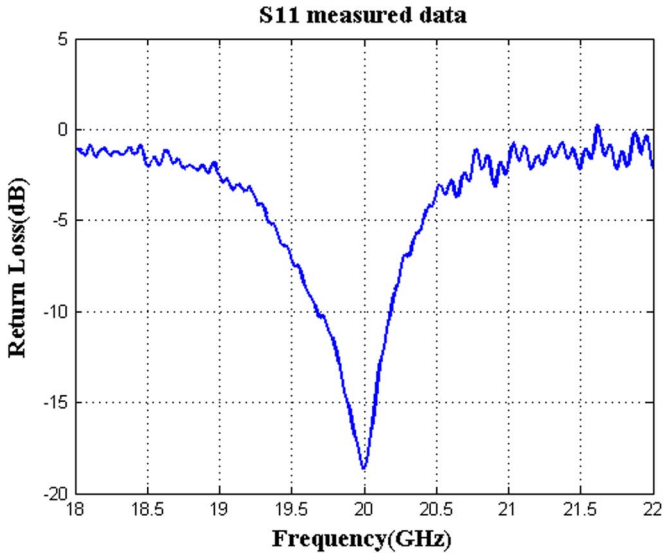

Fig. 8. Measured S_{11} of a 4×4 array antenna without slabs as shown in Fig. 7(a).

The feeding network is a simple one-to-four power divider with $\lambda/4$ impedance matching sections as shown in Fig. 7. Also shown in Fig. 7 are the positions of the dielectric slabs for the 3-bit phase shifter. Although twelve actuators will be required to move them independently, a simple mechanism can be used if this antenna is utilized for the satellite tracking. The input reflection S_{11} is measured with VNWA and shown in Fig. 8. It is better than -15 dB at 20 GHz.

The radiation patterns measured at different phase shift conditions are shown in Figs. 9–13. Fig. 7(a) shows a 4×4 array antenna without the dielectric slabs on it. This corresponds to the no-phase shift among 4 elements, and, therefore, we should expect a beam peak at 0°. Fig. 9 shows the measured and simulated H-plane radiation patterns of this case, and Fig. 10 shows that of E-plane. The simulated and measured E- and H-plane radiation patterns are in agreement. The large sidelobe in E-plane (Fig. 10) may be due to the interference from the feeding network. This can be reduced by placing the CPW and feeding network sections on the bottom side.

Figs. 11 to 13 show the radiation patterns with the phase shift. In all cases, the measured data is normalized with respect to the peak value of the 0° phase shift (Fig. 9). Fig. 11 shows the simulated and measured H-plane radiation patterns with dielectric slabs on a CPW. The phase shifts from left to right are

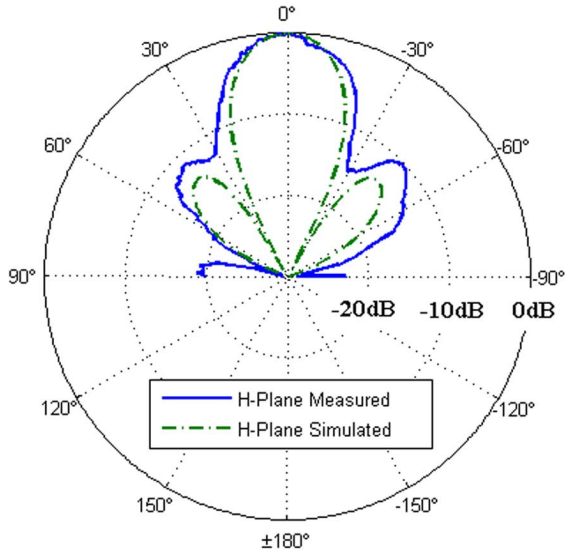

Fig. 9. Simulated and measured H-plane radiation patterns: No phase shift case. Slab positions are (000,000,000,000).

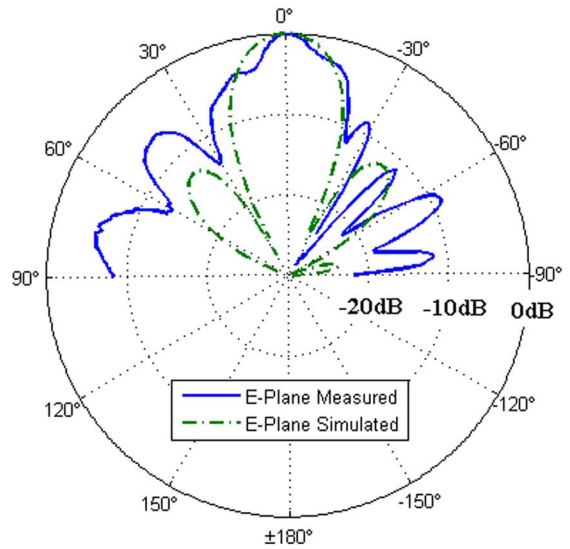

Fig. 10. Simulated and measured E-plane radiation patterns: No phase shift case. Slab positions are (000,000,000,000).

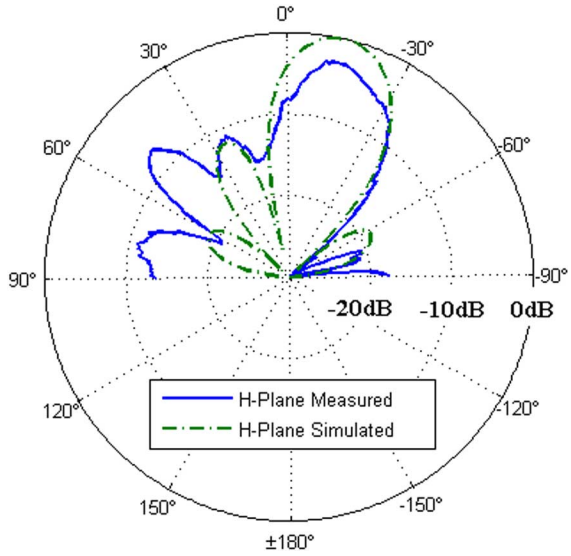

Fig. 11. Simulated and measured H-plane radiation patterns. The phase shift among elements is $-45°$ which corresponds to the beam angle of 15°. Slab positions are (110,010,100,000).

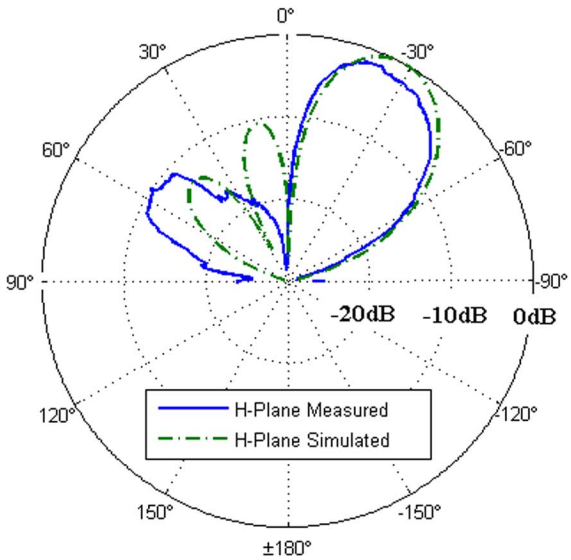

Fig. 12. Simulated and measured H-plane radiation patterns: The phase shift among elements is $-90°$ which corresponds to the beam angle of 30°. Slab positions are (011,001,010,000).

$-135°, -90°, -45°$, and 0° which correspond to the 3-bit patterns of (110,010,100,000). The beam scan angle (peak) is at $-15°$ (345°) for this configuration. Fig. 12 shows the simulated and measured H-plane radiation patterns with dielectric slabs on the CPW. These phase shifts from left to right are $-270°, -180°, -90°$, and 0° which corresponds to the 3-bit patterns of (011,001,010,000). The beam scan angle (peak) is at $-30°$ (330°) for this configuration. Fig. 13 shows the maximum beam scan angle of $+45°$ which can be obtained with $-135°$ phase shifting among elements. From left to right, the phase shift is 0°, $-135°, -270°$, and $-405°$ (45°) with the corresponding 3-bit pattern of (000,110,011,100).

Figs. 9 to 13 are four examples of the eight possible states which can be obtained from a 3-bit phase shifter. Other beam scan angles can be obtained by changing the dielectric slab positions. With this simple setup, the main beam can be scanned from $-45°$ to $+45°$ at 20 GHz. For a 3-bit phase shifter, each CPW has three dielectric slabs. The 4-element array, therefore, requires twelve slabs as illustrated in Fig. 7(b). If arbitrary beam scanning is needed, twelve actuators are required. As a possible application for satellite tracking antennas, whose scan angle can be predicted based on the satellite position, we could use the position-coded rod for each bit. In our case, three rods with notches that press down on the dielectric slabs will be sufficient. By moving all 3 rods simultaneously, we can scan the beam from $-45°$ to $+45°$. This idea will require only one motor. If a 2-D scan is needed for satellite tracking, the rotational stage with another motor will be sufficient. The expected height of this antenna will be relatively thin, and it will basically be a planar 2-D scanning antenna.

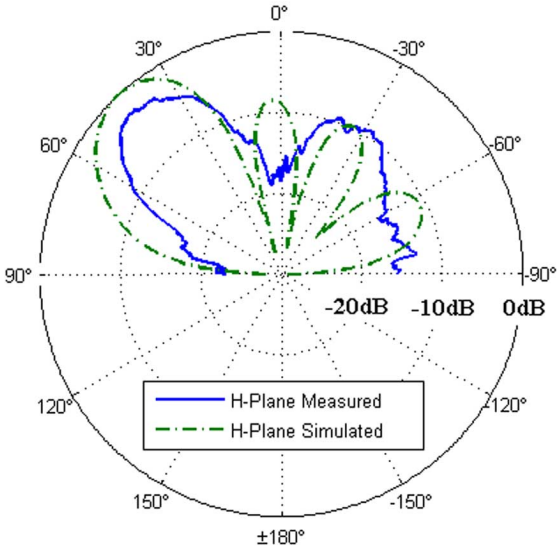

Fig. 13. Simulated and measured H-plane radiation patterns: The phase shift is -135° which corresponds to the beam scan angle of 45°. Slab positions are (000,110,011,100).

IV. Conclusion

The purpose of this paper is to show the feasibility of designing a simple steerable antenna at 20 GHz. Using extensive numerical simulations, we have obtained the desired structure and material to create a 3-bit phase sifter fabricated on an IS640 substrate. The proposed antenna is suited for scanning in one direction such as an indoor/outdoor wireless system. For a satellite tracking antenna which requires a 2-D scan, the rotational motion must be provided by the motor-driven turntable. Although further design work is needed to make a practical system, we have demonstrated that our idea is feasible, and we should be able design a low-cost beam steerable antenna at MMW frequencies. We believe the proposed method is particularly suited for high MMW frequency array antennas for which the solid state-based or MEMS-based phase shifter is difficult and expensive to design [16].

References

[1] R. C. Hansen, *Phased Array Antennas*. New York: Wiley Interscience, 1998.
[2] R. J. Mailloux, *Phased Array Antennas Handbook*. Norwood, MA: Artech House, 1994.
[3] J. S. Hayden and G. M. Rebeiz, "Very low-loss distributed X-band and Ka-band MEMS phase shifters using metal-air-metal capacitors," *IEEE Trans. Microw. Theory Tech.*, vol. 51, no. 1, pp. 309–314, Jan. 2003.
[4] B. Acikel, T. R. Raylor, P. J. Hansen, J. S. Speck, and R. A. York, "A new high performance phase shifter using $BaSrTiO_3$ thin films," *IEEE Microw. Wireless Compon. Lett.*, vol. 12, no. 7, pp. 237–239, Jul. 2002.
[5] S. G. Kim, T. Y. Yun, and K. Chang, "Time-delay phase shifter controlled by piezoelectric transducer on coplanar waveguide," *IEEE Microw. Wireless Compon. Lett.*, vol. 13, no. 1, pp. 19–20, Jan. 2003.
[6] J. Cha, Y. Kuga, and S. Lee, "A continuously steerable array antenna using movable dielectric slabs on a coplanar waveguide," *Microw. Opt. Technol. Lett.*, vol. 48, no. 11, pp. 2222–2227, Nov. 2006.
[7] Y. Kuga, J. Cha, J. A. Ritcey, and T. Kajiya, "Mechanically steerable antennas using dielectric phase shifters," in *IEEE Antennas Propag. Soc. Int Symp. Dig.*, Monterey, CA, Jun. 20–24, 2004, vol. 1, pp. 161–164.
[8] J. Baker-Jarvis and E. J. Vanzura, "Improved technique for determining complex permittivity with the transmission/reflection method," *IEEE Trans. Microw. Theory Tech.*, vol. 38, no. 8, pp. 1096–1101, Aug. 1990.
[9] J. Cha, Y. Kuga, and T. Kajiya, "Mechanically steerable antennas with controllable microwave phase shifters at 20 Ghz," in *IEEE Antennas Propag. Soc. Int Symp. Dig.*, Washington, DC, Jul. 03–06, 2005, vol. 1, pp. 691–694.
[10] K. C. Gupta, R. Garg, I. Bahl, and P. Bhartia, *Microstrip Lines and Slotlines*. Boston, MA: Artech House, 1996.
[11] G. Ghione and C. U. Naldi, "Coplanar waveguide for MMIC applications: Effect of upper shielding, conductor backing, finite-extent ground planess, and line-to-line coupling," *IEEE Trans. Microw. Theory Tech.*, vol. 35, no. 3, pp. 260–267, Mar. 1987.
[12] S. S. Bedair and I. Wolff, "Fast, accurate and simple approximate analytic formulas for calculating the parameters of supported coplanar waveguides for (M)MIC's," *IEEE Trans. Microw. Theory Tech.*, vol. 40, no. 1, pp. 41–48, Jan. 1992.
[13] C. F. Wang, F. Ling, and J. M. Jin, "A fast full-wave analysis of scattering and radiation from large finite arrays of microstrip antennas," *IEEE Trans. Antennas Propag.*, vol. AP-46, pp. 1467–1474, Oct. 1998.
[14] K. L. Wu, M. Spenuk, J. Litva, and D. G. Fang, "Theoretical and experimental study of feed network effects on the radiation patterns of series-fed microstrip antenna arrays," *Proc. Inst. Elect. Eng.*, vol. 138, pt. H, pp. 238–242, June 1991.
[15] E. Levine, G. Malamud, S. Shtrikman, and D. Treves, "A study of microstrip array antennas with the feed network," *IEEE Trans. Antennas Propag.*, vol. AP-37, pp. 426–434, Apr. 1989.
[16] J. Schoebel, T. Buck, M. Reimann, M. Ulm, M. Schneider, A. Jourdain, G. Carchon, and H. A. C. Tilmans, "Design considerations and technology assessment of phased-array antenna systems with RF MEMS for automotive radar applications," *IEEE Trans. Antennas Propag.*, vol. AP-53, pp. 1968–1975, Jun. 2005.

Junho Cha (S'00–M'07) received the B.S. degree in electronics engineering from Kwangwoon University, Seoul, Korea, in 1996 and the M.S. and Ph.D. degrees in electrical engineering from the University of Washington, Seattle, in 1998 and 2006, respectively.

While working toward the Ph.D. degree, he was a Research Assistant at the Electromagnetics and Remote Sensing Laboratory at the University of Washington. Additionally, from 2000 to 2001, he completed an internship at the Workstation Products Division, Intel, Sacramento, CA, where he developed and analyzed SSO/SSN simulations on the electronic packaging. He is currently a Research Associate in the Department of Electrical Engineering at the University of Washington. His research interests are in the areas of microwave and millimeter-wave array antennas, high frequency devices and materials, signal integrity, and numerical and experimental electromagnetics.

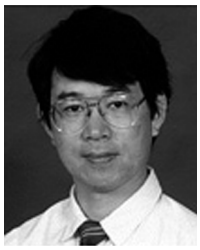

Yasuo Kuga (F'04) received the B.S., M.S., and Ph.D. degrees from the University of Washington, Seattle, in 1977, 1979, and 1983, respectively. His research interests are in the areas of microwave and millimeter-wave remote sensing, high frequency devices and materials, and optics.

He is a Professor of electrical engineering at the University of Washington. From 1983 to 1988, he was a Research Assistant Professor of electrical engineering at the University of Washington. From 1988 to 1991, he was an Assistant Professor of electrical engineering and computer science at The University of Michigan. Since 1991, he is with the University of Washington.

Dr. Kuga was an Associate Editor of *Radio Science* (1993–1996) and IEEE Transactions on Geoscience and Remote Sensing (1996–2000).

Akira Ishimaru (M'58–SM'63–F'73–LF'94) received the B.S. degree from the University of Tokyo, Tokyo, Japan, in 1951 and the Ph.D. degree in electrical engineering from the University of Washington, Seattle, in 1958.

From 1951 to 1952, he was with the Electrotechnical Laboratory, Tanashi, Tokyo, and in 1956, he was with Bell Laboratories, Holmdel, NJ. In 1958, he joined the faculty of the Department of Electrical Engineering of the University of Washington, where he was a Professor of electrical engineering, an Adjunct Professor of applied mathematics and is currently Professor Emeritus. He has also been a Visiting Associate Professor at the University of California, Berkeley. His current research includes waves in random media, remote sensing, object detection, and imaging in clutter environment, inverse problems, millimeter wave, optical propagation and scattering in the atmosphere and the terrain, rough surface scattering, optical diffusion in tissues, and metamaterials. He is the author of *Wave Propagation and Scattering in Random Media* (NewYork: Academic, 1978; IEEE-Oxford University Press Classic reissue, 1997) and *Electromagnetic Wave Propagation, Radiation, and Scattering* (Englewood Cliffs, NJ: Prentice-Hall, 1991). He was Editor (1979–1983) of *Radio Science* and Founding Editor of *Waves in Random Media, Institute of Physics* and *Waves in Random and Complex Media* (Taylor & Francis, U.K.).

Dr. Ishimaru is a Fellow of the Optical Society of America, the Acoustical Society of America, and the Institute of Physics, U.K. He has served as a member-at-large of the U.S. National Committee (USNC) and was Chairman (1985–87) of Commission B of the USNC/International Union of Radio Science. He was the recipient of the 1968 IEEE Region VI Achievement Award and the IEEE Centennial Medal in 1984. He was appointed as Boeing Martin Professor in the College of Engineering in 1993. In 1995, he was awarded the Distinguished Achievement Award from the IEEE Antennas and Propagation Society. He was elected to the National Academy of Engineering in 1996. In 1998, he was awarded the Distinguished Achievement Award from the IEEE Geoscience and Remote Sensing Society. He is the recipient of the 1999 IEEE Heinrich Hertz Medal and the 1999 URSI Dellinger Gold Medal. In 2000, he received the IEEE Third Millennium Medal.

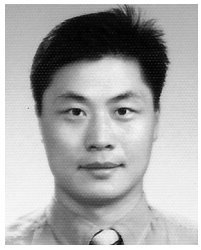

Sangil Lee received the B.E. and M.E. degrees in electronics engineering from Korea University, Seoul, in 1991 and the Ph.D. degree in electrical engineering from the University of Washington, Seattle, in 1994 and 2002, respectively.

He joined Samsung Electronics in 2002, where he worked on fiber-based wireless indoor networks. In 2003, He joined the faculty of the Department of Electronics Engineering, Mokpo National University, Korea. His main research interests are fields of microwave techniques and broadband communications.